available at www.sciencedirect.com

ScienceDirect

journal homepage: www.elsevier.com/locate/agrformet

Diurnal and seasonal variations of UV radiation on the northern edge of the Qinghai-Tibetan Plateau

Xiaoyong Cui [a,b,c], *Song Gu* [a,b], *Xinquan Zhao* [a], *Jing Wu* [c], *Tomomichi Kato* [d], *Yanhong Tang* [b,*]

[a] *Northwest Institute of Plateau Biology, Xining 810008, PR China*
[b] *National Institute for Environmental Studies, 16-2 Onogawa, Tsukuba, Ibaraki 305-8506, Japan*
[c] *College of Resources and Environment, Graduate School of the Chinese Academy of Sciences, Beijing 100049, PR China*
[d] *Frontier Research Center for Global Change 3173-25 Showa-machi, Kanazawa-ku, Yokohama city, Kanagawa 236-0001, Japan*

ARTICLE INFO

Article history:
Received 22 October 2006
Received in revised form
18 June 2007
Accepted 26 September 2007

Keywords:
Alpine meadow
Broadband sensor
Ozone concentration
TOMS

ABSTRACT

We monitored UVA, UVB, and solar radiation from August 2001 to 2003 on the northern Qinghai-Tibetan Plateau to characterize the diurnal and seasonal variations of UV radiation on the world's highest plateau. Daily UVB radiation and the ratio of UVB to total solar radiation increased significantly when the atmospheric ozone concentration decreased as estimated by the total ozone mapping spectrometer (TOMS), as well as when cloud coverage decreased. The UVB/UVA ratio also showed a significant increase when the TOMS ozone concentration decreased in the morning. The seasonal variation pattern of UVB, however, was closely correlated with solar elevation but was little affected by the seasonal pattern of the atmospheric ozone amount. Compared to observations from the central plateau, the magnitude of the UVB increase attributed to ozone depletion was smaller at the northern edge. The study suggests that the temporal variation of ground UV radiation is determined by both solar elevation and the ozone amount, but the spatial difference on the plateau is likely to be ascribed mainly to the spatial variation of the ozone amount.

1. Introduction

Man-made chemicals are considered to have caused world-wide depletion of the atmospheric ozone layer (Pyle, 1997; McKenzie et al., 1999; Wei et al., 2006). Long-term satellite observations have shown that the stratospheric ozone amount is much less over the Qinghai-Tibetan Plateau, particularly in summer, than over other areas with the same latitude (Zhou and Luo, 1994; Zou, 1996; Zheng et al., 2004; Bian et al., 2006). Recent studies indicate that the ozone layer over the plateau is slowly decreasing (Zou, 1996; Liu et al., 2003; Li et al., 2005; Zhang et al., 2006; Zhou et al., 2006).

The depletion of the ozone layer may lead to an increase of ground UVB (Frederick et al., 2000; WMO and UNEP, 2006). Using the ratio of UV radiation to global radiation (UVB/G), Blumthaler and Ambach (1990) found a long-term increase of the incidence of UVB in a mid-latitude alpine region. Measurements in Italy and England indicate that UVB incidence increased with decreasing ozone amount at fixed solar zenith angles (SZA) (Casale et al., 2000; Bartlett and Webb, 2000). In Tibet, a 2 month observation showed an evident increment of UVB radiation that closely corresponded to the declination of stratospheric ozone (Ren et al., 1997, 1999). The UVB intensity at ground-level increased as the total ozone column decreased (Zhang et al., 2003). The World Meteorological Organization (WMO) also suggested that the Qinghai-Tibetan Plateau was a local center with a high UV index (http://toms.gsfc.nasa.gov/ery_uv/euv_v8.html).

* *Corresponding author at*: National Institute for Environmental Studies, Onogawa 16-2, Tsukuba 305-8506, Japan. Tel.: +81 298 50 2481.
E-mail address: tangyh@nies.go.jp (Y. Tang).
0168-1923/$ – see front matter
doi:10.1016/j.agrformet.2007.09.008

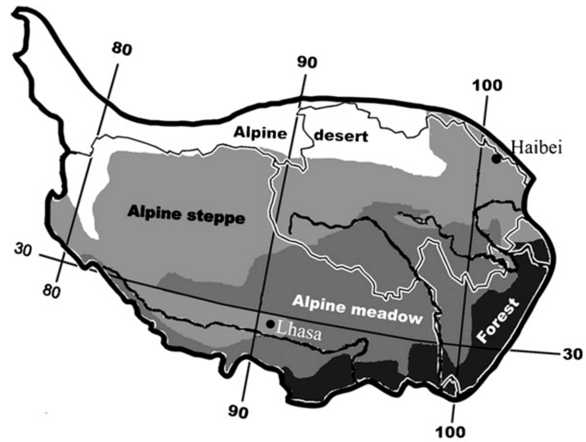

Fig. 1 – Map of the Qinghai-Tibetan Plateau showing the study site and zonal vegetation regions.

Other tropospheric conditions, including aerosol concentration, cloud conditions, and surface albedo, also affect ground-level UV radiation (Li et al., 2000; Alados-Arboledas et al., 2003; Bernhard et al., 2005b; Aculinin, 2006). The Qinghai-Tibetan Plateau has a vast area of more than 2.5×10^6 km^2. It also dramatically variable elevations, ranging from less than 100 m to more than 8844 m, accompanied by drastic spatial heterogeneity of climate, surface status, and vegetation. The plateau precipitation varies by around a factor of 400, sunshine time and cloud time vary by about a factor of 2, and the landscape changes from rain forest to desert (Integrated Survey Team of the Qinghai-Tibet Plateau, 1984). Ground-level UV radiation on the plateau is thus expected to be spatially heterogeneous within the plateau even with the same stratospheric ozone amount. Moreover, satellite observations have shown that the ozone amount is not uniform over the plateau (Zou, 1996; Bian et al., 2006). More ground-based measurements should therefore be conducted to clarify the spatial and temporal patterns of UV radiation in the Qinghai-Tibetan Plateau.

Currently, most UV monitoring sites are distributed around North America, Europe, and Australia (Udelhofen et al., 2000; Martinez-Lozano et al., 2002; Bernhard et al., 2005a; Kimlin et al., 2005). Over the Qinghai-Tibetan Plateau, only very limited information on UV radiation at ground-level is currently available (Ren et al., 1997, 1999). China Global Atmosphere Watch Baseline Observatory at Waliguan (36°17′N, 100°53′E, 3810 m) also monitored UV irradiance from 1991 using an MKII Brewer spectrophotometer (Sci-Tech Instruments, Saskatoon, Canada) and a UVB-1 Broadband pyranometer (Yankee Environmental Systems, Inc., USA). Zhang et al. (2003) has reported on the seasonal variation of UV. Another group has compared short-term UV irradiance among five locations, two of which are in the Qinghai-Tibetan Plateau (Jiang et al., 1998). Here, we report the first observations of UV radiation for the northern plateau (Fig. 1).

The objectives of our study were: (1) to fill in the gaps in UV radiation observation on the vast Qinghai-Tibetan Plateau, (2) to characterize the temporal and spatial variability of UV radiation on the world's highest plateau, and (3) to address how the variability is related to ozone and other variables. We hypothesized that UV radiation should be lower and less temporally variable at the plateau edge (Haibei) than in the center (Lhasa) due to the presence of the stratospheric ozone mini-hole.

2. Material and methods

2.1. Study site and measurements

Measurements were conducted over a *Kobresia humilis* meadow in the Haibei Alpine Meadow Ecosystem Research Station (lat. 37°29′N, long. 101°12′E) at the northeast edge of the Qinghai-Tibetan Plateau at an elevation of approximately 3250 m. Kato et al. (2004) made a detailed description of the site. The annual mean air temperature is −2 °C, and the annual precipitation is 500 mm (Klein et al., 2001). The soil is a clay loam, and its average thickness is 65 cm. The top 5–10 cm of the soil is wet and high in organic matter content. The plant community is dominated mainly by three major perennial sedges, *Kobresia humilis*, *Kobresia pygmaea*, and *Kobresia tibetica* (Cyperaceae). There are a few very small shrubs in the meadow. The plant growing period is from May to October. The maximum aboveground biomass varied within the range of 342 ± 50 g d.w. m^{-2} (average ± S.D.) from 1980 to 1993 during the summer. The LAI (leaf area index) reached a maximum of about four in July. The study site is grazed by yaks and sheep every winter.

UVA and UVB were measured by PD204A and PD204B sensors (Macam Photometrics Ltd., Scotland), respectively. UVA and UVB are generally defined as light with wavelengths of 400–320 and 320–280 nm, respectively. The center wavelengths of the two sensors were approximately 368 and 312 nm with bandwidths of about 30 and 19 nm FWHM (full width at half maximum), respectively. The cosine errors of both sensors are within ± 5% up to 70°. Solar radiation was monitored with a net radiometer CNR-1 (Kipp & Zonen, the Netherlands). All sensors were mounted horizontally on a metal plate 220 cm above the ground. The calibration was performed by the manufacturer before installation in July 2001. No further calibration was done during the 2 years measurement period. To check for significant degradation in sensor sensitivity, we examined the correlations of UVA and UVB with the photosynthetic photon flux density (PPFD) and found no significant difference of the two UV components in relation to the PPFD during this period. The PPFD was monitored by a LI-190SB (Li-cor Inc., USA), which was calibrated with a standard LI-190 (Li-cor Inc.) at least once a year. A CR23X datalogger (Campbell Scientific Inc., USA) was used to record spot data continuously at 15-min intervals. In this study, UV data with solar zenith angle (SZA) below 70° in 2002 and 2003 were used for analysis.

2.2. Modeling solar radiation and classification of cloud amount

Solar global radiation can be obtained from different models. Models such as SMARTS1 (simple dispersion model, Gueymard, 2001) and SBDART2 (multiple dispersion model, Ricchiazzi et al., 1998) can provide precise results, but they require many parameters that are not available for the current study. We therefore decided to use a classic model that obtains solar radiation (Jones, 1992) and also meets the objectives of the current study, as follows:

$$R_{dir} = R_0 \tau^n \sin\theta \quad (1)$$

$$R_{dif} = R_0 0.5(1 - \tau^n)\sin\theta \quad (2)$$

$$n = \frac{P/P_0}{\sin\theta} \quad (3)$$

where R_{dir} and R_{dif} are the direct and diffuse solar radiation, respectively; R_0 the solar constant above the atmosphere, 1367 W m^{-2}; τ the atmospheric extinction coefficient, 0.84 for clear air; P the ambient air pressure; and P_0 is the standard air pressure at sea level, 101.3 kPa. The solar elevation angle θ is calculated by

$$\sin\theta = \sin\lambda\sin\delta + \cos\lambda\cos\delta\cos\eta \quad (4)$$

where λ, η, and δ represent latitude, hour angle, and solar declination of the respective day, respectively. η and δ are calculated as follows:

$$\eta = \frac{15\pi(T - T_{sn})}{180} \quad (5)$$

$$\delta = 23.45\cos\left[\frac{2\pi(D - 172)}{365}\right]\frac{\pi}{180} \quad (6)$$

where T and D are the time of day and the day of the year (DOY), respectively. T_{sn} denotes the standard noon time. The datalogger was adjusted to Beijing Standard Time (BST, 120°E), therefore

$$T_{sn} = \frac{12 + (120 - 101.2)}{15} \approx 13.25 \text{ BST} \quad (7)$$

Cloud transmission is calculated by

$$T_r = \frac{R}{R_{dir} + R_{dif}} \quad (8)$$

where R is the measured solar radiation. A clear sky requires a T_r greater than 0.85 in this study. The definition for "clear sky transmissivity" varies depending on location (latitude, longitude, and elevation), time (time of day and DOY), and atmospheric conditions. Smith (1991) set 0.75 as the clear sky index, and Oke (1987) suggested 0.85. Values between 0.70 and 0.91 have been reported for different conditions (Nardino et al., 2000; Mayer and Kylling, 2005; van den Broeke, 2005; Wendler, 2005; Key and Minnett, 2006). We determined the transmissivity to be 0.85 in agreement with Oke (1987) because Oke's alpine site was at a high elevation and had relatively clear skies in common with the Tibetan Plateau.

2.3. Stratospheric ozone amount and UV radiation data from TOMS

The daily ozone amount; daily UV doses at 305, 315, 325, and 380 nm; and the UVER (UV radiation weighted by the action spectrum for the erythema) dose at noon were downloaded from http://toms.gsfc.nasa.gov/ for the study site. UVER was also calculated by linear regression based on measured UVA and UVB at noon.

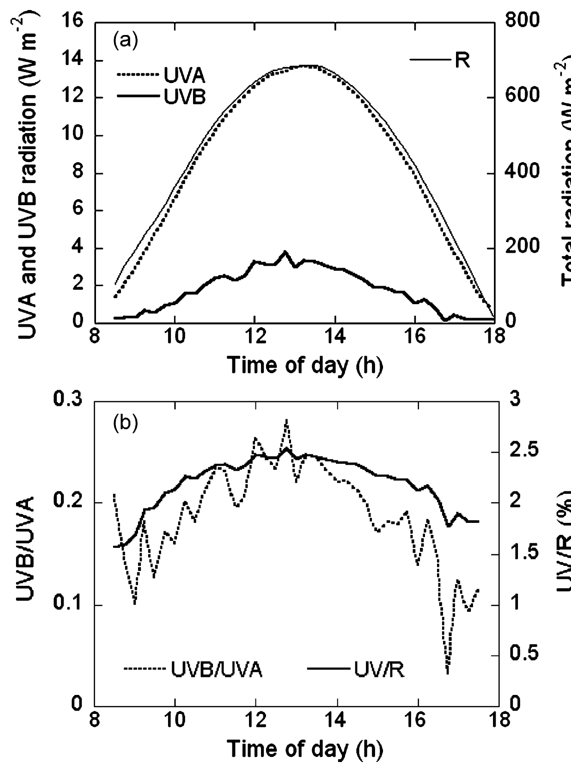

Fig. 2 – Diurnal change of (a) UVA, UVB, and total solar radiation and (b) ratios of UV radiation to total solar radiation and UVB/UVA on a clear day, 11 November 2002.

3. Results and discussion

3.1. Diurnal variation of UV radiation

UV radiation showed the same diurnal pattern as total solar radiation on clear days (e.g., 11 November 2002, Fig. 2a). All of

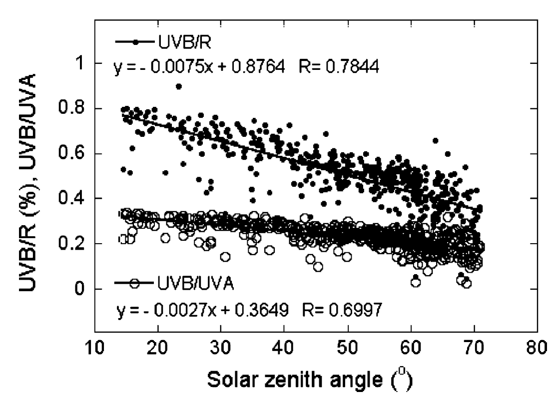

Fig. 3 – Changes of UVB/R and UVB/UVA with solar zenith angle (SZA) from all clear days in 2002. Data for SZAs greater than 70° were excluded due to the effect of high noise on the small values of solar radiation and UVA.

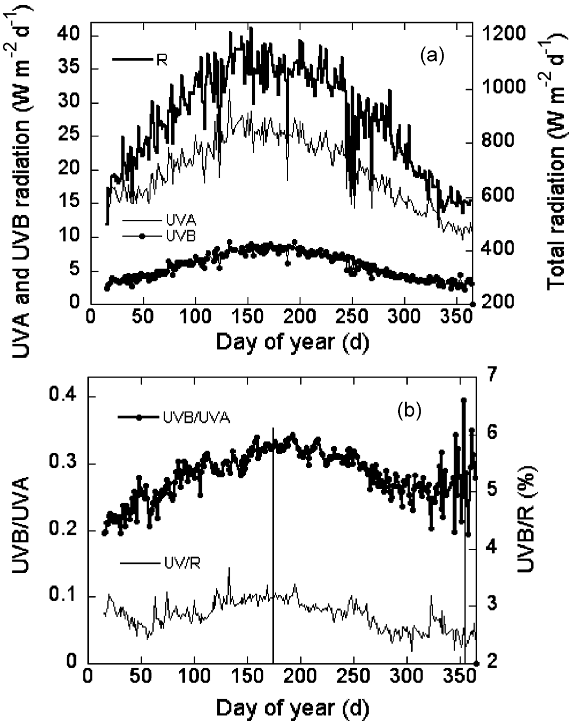

Fig. 4 – Seasonal variation of (a) daily total UVA, UVB, and solar radiation, and (b) the midday UV/R and UVB/UBA in 2002. The vertical lines in (b) indicate DOYs 172 and 353.

the variables reached their daily maximum at local noon time, about 13:25 BST. The ratio of UV radiation to total solar radiation (*R*) changed synchronically with total solar radiation and reached its maximum at noon, as did the UVB/UVA ratio (Fig. 2b). UV radiation, particularly UVB radiation measured by the PD204B sensor, showed a more conspicuous increase at midday than did the total solar radiation. The middle day maxima of UV, UVB, and total solar radiation were almost 10, 12, and 6 times higher than the early morning values (taken at about 8:30 BST), respectively (Fig. 2a). This indicates that UV radiation, particularly UVB radiation, has a higher sensitivity than the total solar radiation to the diurnal change of optical path.

On a typical clear day in winter, the incident UV radiation represented only about 2% of the total solar radiation on an energy basis. Regarding UV radiation, the UVB energy was only 20% that of UVA (Fig. 2b). The ratio of UV radiation to total solar radiation varied during the day. Daily average UVB/UVA and UVB/R values decreased significantly ($p < 0.001$) with increasing SZA (Fig. 3). These results indicate that UVB is more rapidly attenuated at large SZAs. A similar result has been reported for Lhasa (Ren et al., 1997).

3.2. *Seasonal variation of UV radiation and its relation to ozone amount*

In the current study, the seasonal pattern of surface UVB is shown to follow the seasonal pattern of the SZA (Fig. 4). We understand that the seasonal variation pattern of ground-level UV radiation should be determined by the SZA and the

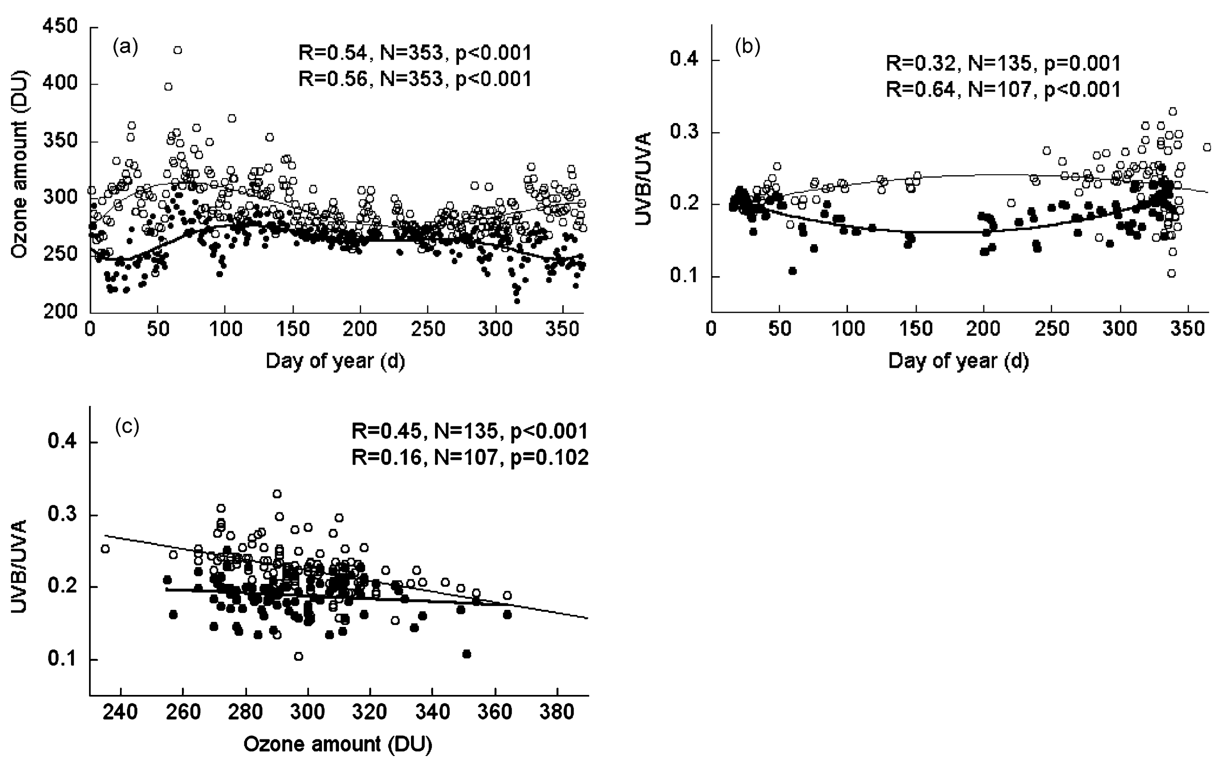

Fig. 5 – Seasonal changes of (a) ozone amount and (b) UVB/UVA, and (c) the relationship between ozone amount and UVB/UVA in Haibei in the morning (○) and afternoon (●) on clear days (cloud transmissivity > 0.85) in 2002. Ozone amount in Lhasa (●) is also plotted in (a) in comparison with Haibei (○). Ozone amount data were downloaded from http://toms.gsfc.nasa.gov/. The curves in (a), (b), and (c) are from 6-order polynomial, linear, and 2-order polynomial models, respectively.

stratospheric ozone amount. If the seasonal pattern of UV radiation follows in parallel with the seasonal pattern of the SZA, there are three possible explanations: (1) there is no seasonal change in the ozone amount; (2) the seasonal pattern of the ozone amount parallels or synchronizes with the seasonal variation of the SZA; or (3) there is a seasonal change of the ozone amount, but the change is counteracted by some unknown atmospheric conditions. Among the three speculations, we can exclude the first one because observations have frequently indicated that there are significant changes in ozone amounts over the Qinghai-Tibetan Plateau (Zhou and Luo, 1994; Zou, 1996; Zheng et al., 2004; Lin and Yao, 2005; Bian et al., 2006). There is also no evidence indicating the existence of the counteracting factors mentioned in the third choice. Therefore, the second speculation is highly probable. Zou (1996) reported that the seasonal pattern of ozone amount exhibited an annual maximum in March and a minimum in October for the period from 1978 to 1991.

We further examined the spatial features in relation to the temporal patterns of UV radiation and ozone amount. Ozone observations show that the seasonal ozone cycle is essentially synchronized with the solar cycle, with a minimum in July and a maximum in late spring. This is different from the site at Lhasa on the other side of the plateau, where the ozone minimum is observed in October and the maximum in March (Fig. 5a). This is consistent with the results from regional analyses of satellite ozone data (Zhang et al., 2003; Lin and Yao, 2005; Bian et al., 2006; Zhou et al., 2006). The difference between Lhasa and Haibei was larger in winter than in summer. Significant linear correlations occurred between ozone amount and the ratio of UVB/UVA in the morning but not in the afternoon (Fig. 5c). UVB/UVA was higher in the morning than it was in the afternoon at the same SZA, particularly in summer when the amount of ozone was low (Fig. 5b). This may be due to the more frequent cloud cover in the afternoon than in the morning, especially during the summer monsoon season, as was also observed in Lhasa (Ren et al., 1997).

The intensity of UVA and total UV radiation in summer was about three times higher than in winter. The magnitude of the seasonal difference was similar to that reported for lowland areas at the same latitude (e.g., in Tokyo and Tsukuba, http://www-cger2.nies.go.jp/ozone/uv/uv_index/tsukuba/index.html, and in Shonan, http://www.shonan-it.ac.jp/each_science/info/uvobs/, in Japanese language) but somewhat lower than that in Lhasa (Ren et al., 1999). Since the seasonal pattern of UV radiation was principally determined by the SZA, a higher ratio of summer to winter UV radiation is expected to be observed in higher latitudes (e.g., in England, see Bartlett and Webb, 2000; and in Norway, see Johnsen et al., 2002). Therefore, the lower ratio of summer to winter UV radiation observed at the higher latitude Haibei than at the lower latitude Lhasa was probably not caused by the latitude difference but may have been caused by the ozone column being lower in the center than in the edge area of the Qinghai-Tibetan Plateau.

3.3. *Effect of cloud amount on UV radiation*

The attenuating effects of cloud cover on UVA and UVB radiation have been demonstrated to be similar in magnitude (Stamnes et al., 1991). In addition, cloud cover has a greater effect on UV radiation at higher SZA, and the effect tends to be insensitive to SZAs below 20° (Stamnes et al., 1991). By comparing days with different cloud amounts, we found that UVB/R decreased with increasing cloud transmission (Fig. 6a and b). Seasonal data demonstrate a similar trend for UVB/R as well as a slightly higher attenuation of UVA than UVB by cloud cover (Fig. 6c). To eliminate the effect of SZA, we examined the data within the narrow SZA range of $60 \pm 0.5°$. The ozone amount varied greatly during these days where SZA was within $60 \pm 0.5°$ (Fig. 6c). A stepwise regression showed that UVB/R and UVB/UVA were linear functions of cloud transmission and ozone amount. That is, both ozone amount and cloud coverage contributed significant parts to the variation of UVB/UVA ($p < 0.001$ for both variables). For UVB/R, ozone was only marginally significant ($p = 0.048$ in a partial correlation analysis with fixed cloud transmission) while cloud coverage played the major role ($p < 0.001$).

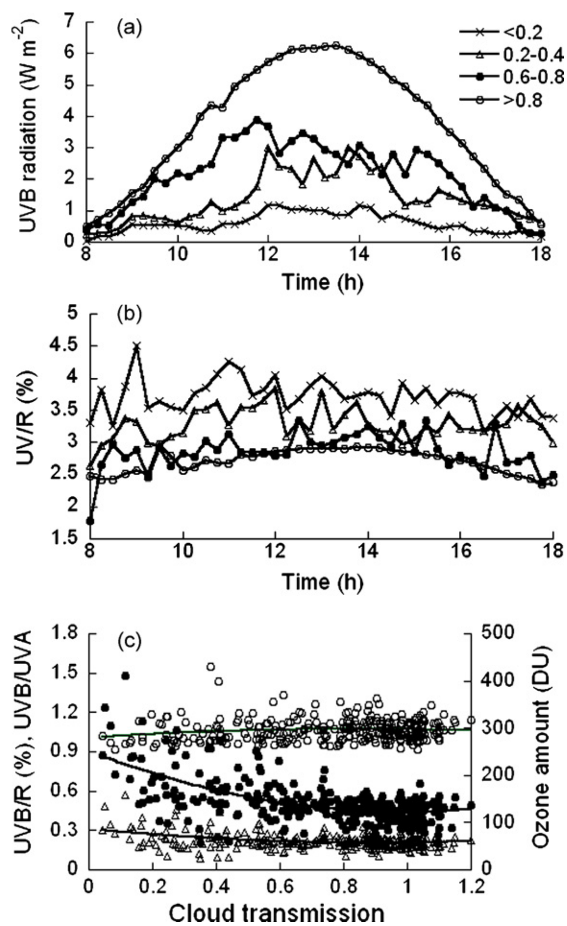

Fig. 6 – Comparisons of (a) UVB radiation intensity and (b) UVB/R with different cloud coverages (indicated by the cloud transmission values in the legend in (a)). The ozone amounts were similar while the minimum SZA varied from 22.5° to 39.4° in these days. (c) Relationships between UVB/R (●), UVB/UVA (△), and ozone amount (○) with cloud cover for seasonal data with SZA within $60 \pm 0.5°$ in 2002. The curves in (c) are 2-order polynomials and all significant ($p < 0.001$ for UVB/R and UVB/UVA and $p = 0.001$ for ozone amount).

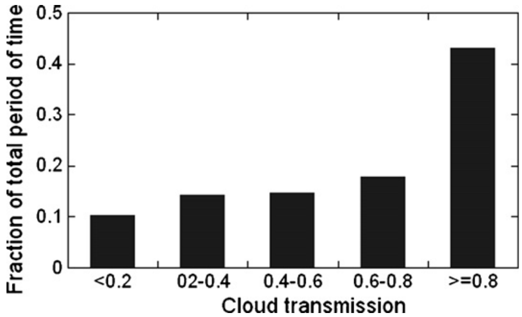

Fig. 7 – Frequency distribution of cloud cover transmittance rate in Haibei from 9:00 to 15:00 during the growth season in 2002.

Fig. 5b indicates that there is likely greater cloud coverage in summer when solar radiation and UVB radiation are high (Fig. 4a). Broken cumulus clouds commonly appear in the afternoon and result in a lower UVB radiation than in the morning (Fig. 5b and c). We estimated that, during the growing season in 2002, Haibei was covered by clouds about 60% of the period between 9:00 and 15:00 local time, with cloud transmission below 0.8 (Fig. 7). Clouds may be much more responsible for the variance of UV radiation than ozone (Bernhard et al., 2005b). The effect of clouds on UV irradiance depend on cloud amount; for instance, it has been reported that clouds reduced UV radiation by 28–90% at Palmer Station, Antarctica (Alados-Arboledas et al., 2003; Bernhard et al., 2005b). Therefore, in addition to alleviating low-humidity and high-radiation stresses (Cui et al., 2003), cloud cover should be considered in the study of the effects of UVB radiation on alpine ecosystems in the plateau.

3.4. *Effectiveness of broadband UV sensors in long-term monitoring*

There are three main types of instruments for ground-based UV measurements: spectroradiometers, multichannel radiometers, and broadband UV sensors. Spectroradiometers measure the entire UV spectrum and/or the ultraviolet erythema radiation (UVER) dose (Stamnes et al., 1991; Bernhard et al., 2005a). Data from multi-channel radiometers can be matched with those from spectroradiometers and determine the UVER dose by linear regression (Dahlback, 1996; Bernhard et al., 2005a). Broadband sensors are the cheapest among the three types of instruments. Some, such as the 7841 UV sensor (Davis Instruments, USA), can measure the UVER dose directly, but most do not directly yield the UVER dose (Bodhaine et al., 1998; Aculinin, 2006). Broadband sensors show large discrepancies with the other two types of instruments (Johnsen and Hannevik, 1997; Zhang et al., 2003; Bernhard et al., 2005a). Nevertheless, errors of up to 20% are not uncommon even in spectroradiometer measurements (Jokela et al., 2000). All three types of instruments from various manufacturers are used worldwide (Webb, 1997, 2003).

The UV sensors we used respond to UV radiation with a spectrum feature different from an erythema UV response. Hence, it is not possible to determine the UVER dose directly from these UV sensors (Alados-Arboledas et al., 2003; Seckmeyer et al., 2005). Dahlback (1996) reported a simple method to obtain the UVER dose from measurements with

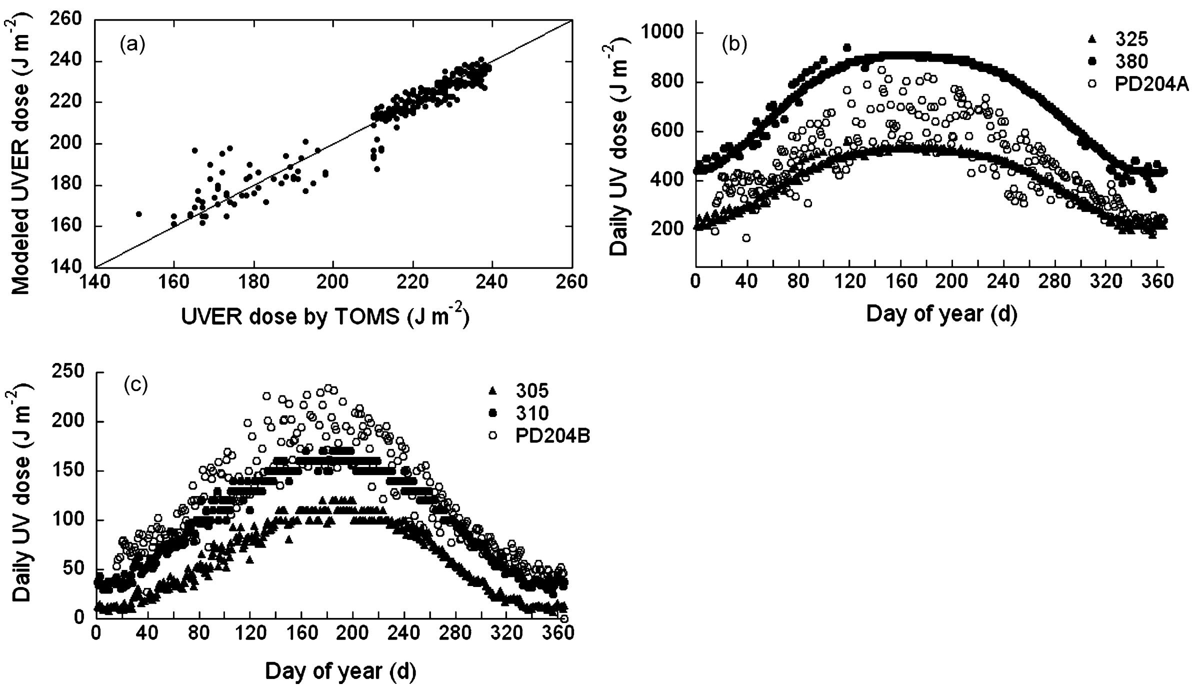

Fig. 8 – (a) Comparison of erythema UV dose at noon provided by TOMS with that calculated from the measured UVA and UVB in this study in 2002 and the seasonal change of daily UV dose by TOMS (305, 310, 325, and 380 nm) compared with those by (b) PD204A and (c) PD204B. The linear models in (a) were y = 203.595 − 1.454UVA + 8.391UVB from DOY 46 to 317 and y = 105.907 + 3.105UVA + 9.449UVB on other days.

multi-channel radiometers. In this method, a radiative transfer model and calibration of the results with spectroradiometers are required. We found that a linear combination of UVA and UVB can make a good prediction of the UVER dose calculated from TOMS spectroradiometry (Fig. 8a). Therefore, these two UV sensors could be used to obtain the UVER dose. Ground-based sensors have advantages over TOMS spectroradiometry in that the former can monitor UV radiation at a particular site continuously and provide information on the climatic effects on UV radiation.

By comparing with spectral data from TOMS, we concluded that the PD204B sensor tends to overestimate UVB radiation and the PD204A sensor tends to underestimate UVA radiation (Fig. 8b, c). This is because the PD204B sensor is insensitive to UV below 300 nm but responds to part of the UVA region with a relative response of 90% at 315 nm, whereas the PD204A sensor is insensitive to UV radiation below 345 or above 385 nm and has a relative response of only 30% within the spectrum range. This means that UVB obtained from the PD204B includes some UVA; the sensitivity of UVB measured by the PD204B in response to ozone variation thus should be lower than that of pure UVB. Nevertheless, variation of UVB with changing ozone amount and cloud cover was evident and the pattern was similar to that reported in other studies (Ren et al., 1997, 1999). Therefore, the two sensors used in the study are applicable for UV measurement if a calibration with a spectroradiometer is conducted.

4. Conclusion

Using broadband UV sensors, we successfully monitored and characterized the temporal variation of UV radiation on the northern edge of the Qinghai-Tibetan Plateau. Ground-based measurements were consistent with satellite data on clear days, indicating that the broadband UV sensors used in the study can make effective measurements of UV radiation at ground-level. The results provide the first detailed reference for understanding the characteristics of diurnal and seasonal variations of the UV environment on the world's highest plateau. Observations in the present study suggest that UV radiation is much lower at the northern edge than in the central plateau.

Acknowledgements

This study was part of a joint research project between the National Institute for Environmental Studies, Japan, and the Northwest Institute of Plateau of Biology, China, supported by the projects "*Integrated Study for Terrestrial Carbon Management of Asia in the 21st Century Based on Scientific Advancements*" and "*Early detection and prediction of climate warming based on the long-term monitoring of alpine ecosystems on the Tibetan Plateau*". The study was also partly supported by the Natural Science Foundation of China (30670318). We declare that the experiments reported in this paper complied with the current laws of the People's Republic of China in which the experiments were performed. We also extend our appreciation to NASA for its valuable data.

References

Aculinin, A.A., 2006. Total column ozone and solar UV-B erythemal irradiance over Kishinev Moldova. Glob. NEST J. 8, 204–209.

Alados-Arboledas, L., Alados, I., Foyo-Moreno, I., Olmo, F.J., Alcántara, A., 2003. The influence of clouds on surface UV erythemal irradiance. Atmos. Res. 66, 273–290.

Bartlett, L.M., Webb, A.R., 2000. Changes in ultraviolet radiation in the 1990s: spectral measurements from Reading, England. J. Geophys. Res. 105, 4889–4893.

Bernhard, G., Booth, C.R., Ehramjian, J.C., 2005a. Real-time ultraviolet and column ozone from multichannel ultraviolet radiometers deployed in the National Science Foundation's ultraviolet monitoring network. Opt. Eng. 44 (4), 041011–41012.

Bernhard, G., Booth, C.R., Ehramjian, J.C., 2005b. UV climatology at Palmer station, Antarctica, based on Version 2 NSF network data. In: Bernhard, G., Slusser, J.R., Herman, J.R., Gao, W. (Eds.), Proceedings of the SPIE, Ultraviolet Ground- and Space-based Measurements, Models, and Effects, 5886(07), pp. 1–12. doi:10.1117/12.614172.

Bian, J., Wang, G., Chen, H., Qi, D., Lu, D., Zhou, X., 2006. Ozone mini-hole occurring over the Tibetan Plateau in December 2003. Chin. Sci. Bull. 51, 885–888.

Blumthaler, M., Ambach, W., 1990. Indication of increasing solar ultraviolet-B radiation flux in alpine regions. Science 248, 206–208.

Bodhaine, B.A., Dutton, E.G., Mckenzie, R.L., Johnston, P.V., 1998. Calibrating broadband UV instruments: ozone and solar zenith angle dependence. J. Atmos. Oceanic Technol. 15, 916–926.

Casale, G.R., Meloni, D., Miano, S., Palmieri, S., Siani, A.M., 2000. Solar UV-B irradiance and total ozone in Italy: fluctuations and trends. J. Geophys. Res. 105, 4895–4901.

Cui, X., Tang, Y., Gu, S., Nishimura, S., 2003. Photosynthetic depression in relation to plant architecture in two alpine herbaceous species. Environ. Exp. Bot. 50, 125–135.

Dahlback, A., 1996. Measurements of biologically effective UV doses, total ozone abundances, and cloud effects with multichannel, moderate bandwidth filter instruments. Appl. Opt. 35, 6514–6521.

Frederick, J.E., Slusser, J.R., Bigelow, D.S., 2000. Annual and interannual behavior of solar ultraviolet irradiance revealed by broadband measurements. Photochem. Photobiol. 72, 488–496.

Gueymard, C., 2001. Parameterized transmittance model for direct beam and circumsolar spectral irradiance. Solar Energy 71, 325–346.

Integrated Survey Team of the Qinghai-Tibet Plateau, 1984. Tibetan Climate. Science Press, Beijing (in Chinese).

Jiang, H., Ji, G., Shi, S., Beng, G., Han, F., 1998. The characteristics of ultraviolet radiation variation over the northern Tibetan Plateau. Acta Energiae Solaris Sinica 19, 7–12.

Johnsen, B.J., Hannevik, M. (Eds.), 1997. The 1995 intercomparison of UV- and PAR instruments at the University of Oslo. StrålevernRapport 1997:7. Østerås, Norwegian Radiation Protection Authority, Norway.

Johnsen, B.J., Mikkelborg, O., Hannevik, M., Nilsen, L.T., Saxebol, G., Blaasaas, K.G., 2002. Norwegian UV monitoring program. Period 1995/1996 to 2001. StrålevernRapport 2002:4. Østerås, Norwegian Radiation Protection Authority, Norway.

Jokela, K., Ylianttila, L., Visuri, R., Leszczynski, K., Kärhä, P., Ikonen, K., 2000. Intercomparison of lamp and detector-based UV-irradiance scales for solar radiometry. J. Geophys. Res. 105, 4821–4827.

Jones, H.G., 1992. Plants and Microclimate: A Quantitative Approach to Environmental Plant Physiology, 2nd ed. Cambridge University Press, Cambridge.

Kato, T., Tang, Y., Gu, S., Cui, X., Hirota, M., Du, M., Li, Y., Zhao, X., Oikawa, T., 2004. Carbon dioxide exchange between the atmosphere and an alpine meadow ecosystem on the Qinghai-Tibetan Plateau, China. Agric. Forest Meteorol. 124, 121–134.

Key, E.L., Minnett, P.J., 2006. Implications of shortwave cloud forcing and feedbacks in the Southern Ocean. Annal. Glaciol. 44, 15–22.

Kimlin, M.G., Slusser, J.R., Schallhorn, K.A., Lantz, K., Meltzer, R.S., 2005. Comparison of ultraviolet data from colocated instruments from the U.S. EPA Brewer Spectrophotometer Network and the U.S. Department of Agriculture UV-B Monitoring and Research Program. Opt. Eng. 44, 041009–41016.

Klein, J., Harte, J., Zhao, X., 2001. Global change research from the Rocky Mountains to the Qinghai-Tibet Plateau: implications for ecosystem carbon storage. In: Zhen, D., Zhu, L. (Eds.), Formation and Evolution, Environmental Change and Sustainable Development on Tibetan Plateau. Academy Press, Beijing, pp. 305–315.

Li, C., Hu, J., Xu, J., Lin, W., Zhao, L., 2005. Prediction on the influence of ozone depletion substance to the stratospheric ozone. Chin. Environ. Sci. 25 (2), 142–145 (in Chinese with English abstract).

Li, Z., Wang, P., Cihlar, J., 2000. A simple and efficient method for retrieving surface UV radiation dose rate from satellite. J. Geophys. Res. 105, 5027–5036.

Lin, W., Yao, B., 2005. Analysis on the vertical ozone profiles over Tibetan Plateau using SAGEIIdata. Res. Environ. Sci. 18 (4), 102–106.

Liu, Y., Li, W., Zhou, X., He, J., 2003. Mechanism of formation of the ozone valley over the Tibetan Plateau in summer-transport and chemical process of ozone. Adv. Atmos. Sci. 20, 103–109.

Martinez-Lozano, J.A., Marín, M.J., Tena, F., Utrilla, M.P., Sánchez-Munlosguren, L., Gonzalez-Fría, C., Cueves, E., Redondas, A., Lorente, J., de Cabo, J., Chamorro, V., Vergez, R., de Frutos, A., Díaz, J.P., Expósito, F.J., de la Morena, B., Vilaplana, J.M., 2002. UV index experimental values during the years 2002 and 2001 from the Spanish broadband UV-B radiometric network. Photochem. Photobiol. 76, 181–187.

Mayer, B., Kylling, A., 2005. Technical note: the libRadtran software package for radiative transfer calculations—description and examples of use. Atmos. Chem. Phys. 5, 1855–1877.

McKenzie, R., Connor, B., Bodeker, G., 1999. Increased summertime UV radiation in NewZealand in response to ozone loss. Science 285, 1709–1711.

Nardino, M., Orsini, A., Pirazzini, R., Calzolari, F., Georgiadis, T., Levizzani, V., 2000. Cloud radiative forcing and effects on local climate. In: Proceedings of the Third European Conference on Applied Climatology, ECAC 2000, Pisa, Italy, October 16–20.

Oke, T.R., 1987. Boundary Layer Climates, 2nd ed. Methuen, NY.

Pyle, J.A., 1997. Global ozone depletion: observations and theory. In: Lumsden, P. (Ed.), Plants and UV-B: Response to Environmental Change. Cambridge University Press, Cambridge, pp. 3–11.

Ci, R.P.B, Gjessing, Y., Sigernes, F., 1999. Measurements of solar ultra violet radiation on the Tibetan Plateau and comparison with discrete ordinate method simulations. J. Atmos. Solar Terres. Phys. 61, 425–446.

Ci, R.P.B, Sigernes, F., Gjessing, Y., 1997. Ground-based measurements of solar ultraviolet radiation in Tibet: preliminary results. Geophys. Res. Lett. 24, 1359–1362.

Ricchiazzi, P., Yang, S., Gautier, C., Sowle, D., 1998. SBDART: a research and teaching software tool for plane-parallel radiative transfer in the earth's atmosphere. Bull. Am. Meteorol. Soc. 79, 2101–2114.

Seckmeyer, G., Bais, A., Bernhard, G., Blumthaler, M., Booth, C.R., Lantz, K., McKenzie, R.L., Wuttke, S., Smolskaia, I., 2005. Broadband instruments measuring erythemally weighted solar irradiance—the new WMO UV instrumentation document. Geophys. Res. 7, 08927 (abstract).

Smith, M., 1991. Report on the expert consultation on procedures for revision of FAO guidelines for prediction of crop water requirements. Food Agric. Org. U.N., Rome, Italy.

Stamnes, K., Slusser, J., Bowen, M., 1991. Derivation of total ozone abundance and cloud effects from spectral irradiance measurements. Appl. Opt. 30, 4418–4426.

Udelhofen, P.M., Gies, H.P., Roy, C.R., 2000. Comparison of measurements of surface UVR and TOMS UV exposures over Australia. In: Proceedings of the SPARC 2000 Second General Assembly of the SPARC/WCRP Project. Mar Del Plata, Argentina, November 6–10.

van den Broeke, M., 2005. Strong surface melting preceded collapse of Antarctic Peninsula ice shelf. Geophys. Res. Lett. 32, L12815, doi:10.1029/2005GL023247.

Webb, A.R., 1997. Monitoring changes in UV-B radiation. In: Lumsden, P. (Ed.), Plants and UV-B: Response to Environmental Change. Cambridge University Press, Cambridge, pp. 13–30.

Webb, A.R., 2003. UV instrumentation for field and forest research. Agric. Forest Meteorol. 120, 27–38.

Wei, K., Chen, W., Huang, R., 2006. Long-term changes of the ultraviolet radiation in China and its relationship with total ozone and precipitation. Adv. Atmos. Sci. 23, 700–710.

Wendler, G., 2005. UV radiation in the southern seas in summer 2000. In: Proceedings of the Eighth Conference on Polar Meteorology and Oceanography, San Diego, USA, January 9–13.

WMO and UNEP, 2006. Executive Summary: WMO/UNEP Scientific Assessment of Ozone Depletion. Prepared by the Scientific Assessment Panel of the Montreal Protocol on Substances That Deplete the Ozone Layer.

Zhang, X., Zheng, X., Tang, J., 2003. Analyses of atmospheric total ozone and UV-B observation characteristics in Mountain Waliguan over the Tibetan Plateau. Qinghai Meteorol. 2, 39–44 (in Chinese).

Zhang, Z., Bian, J., Chen, H., Wang, Z., 2006. Analyze and verify variation features of total atmospheric ozone in mountain Waliguan based on comparison between Brewer and TOMS Data. Clim. Environ. Res. 11, 451–456.

Zheng, X., Zhou, X., Tang, J., Qin, Y., Chan, C., 2004. A meteorological analysis on a low tropospheric ozone event over Xining North Western China on 26–27 July 1996. Atmos. Environ. 38, 261–271.

Zhou, X., Li, W., Chen, L., Liu, Y., 2006. Study on ozone change over the Tibetan Plateau. Acta Meterorol. Sinica 20 (2), 129–143.

Zhou, X., Luo, C., 1994. Ozone valley over Tibetan Plateau. Acta Meteorol. Sinica 8, 505–506 (in Chinese with English abstract).

Zou, H., 1996. Seasonal variation and trends of TOMS ozone over Tibet. Geophys. Res. Lett. 23, 1029–1032.